23

23. STUDIES OF VARIOUS FACTORS AFFECTING DRAG DUE TO LIFT AT SUBSONIC SPEEDS

By William P. Henderson
NASA Langley Research Center

SUMMARY

Studies of various factors affecting the subsonic drag due to lift of thin highly swept wings indicate that wings having sharp leading edges exhibit low values of leading-edge suction, and no significant change in the suction is evident with increasing Reynolds number. Wings incorporating leading-edge radii exhibit 90-percent suction at Reynolds numbers (based on leading-edge radius) above 20 000. The suction developed by highly swept wings falls off considerably with lift coefficient even at relatively high Reynolds numbers, and realistic drag estimates should include this effect. Additional systematic studies are needed to assess the effects of Mach number on leading-edge suction.

INTRODUCTION

Because of the highly swept and relatively sharp leading edges for wing designs of interest for supersonic aircraft such as the proposed supersonic transport, a knowledge of the various factors affecting the drag due to lift at subsonic speeds is becoming increasingly necessary. In view of this interest, an investigation was conducted to determine the effects of Reynolds number, lift coefficient, and wing leading-edge radius on the drag due to lift of a series of thin, highly swept, low-aspect-ratio wing-body configurations. The purpose of this discussion is to review some of the results of this investigation.

SYMBOLS

A	aspect ratio
b	wing span
c	wing chord
$\bar{c}$	mean geometric chord
C_D	drag coefficient
ΔC_D	drag due to lift
$C_{D,i}$	induced drag coefficient
$C_{D,o}$	drag coefficient at zero lift

Preceding page blank

$C_{D,p}$	profile drag coefficient due to lift
$\frac{\partial C_{D,i}}{\partial C_L^2}$	drag-due-to-lift parameter
C_L	lift coefficient
$C_{L,opt}$	optimum lift coefficient
C_N	normal-force coefficient
C_s	suction force coefficient
F	resultant force vector
$(L/D)_{max}$	maximum lift-drag ratio
M	Mach number
$R_{\bar{c}}$	Reynolds number based on $\bar{c}$, $\rho V \bar{c}/\mu$
R_{le}	Reynolds number based on r, $\rho V_n r/\mu$
r	average leading-edge radius
s	leading-edge-suction parameter
V	free-stream velocity
V_n	velocity component measured normal to wing leading edge, $V \cos \Lambda$
y	spanwise coordinate
α	angle of attack
α_i	induced angle of attack
Γ	circulation strength
δ_f	leading-edge flap deflection (positive leading edge up), deg
Λ	wing leading-edge sweep angle, deg
μ	coefficient of viscosity
ρ	density

DISCUSSION

Scope of Investigation

The scope of this wind-tunnel investigation is shown in figure 1. The test conditions provide for Mach numbers less than 0.3 and Reynolds numbers (based on the wing mean-geometric chord) ranging from about 1×10^6 to 20×10^6. The wings, which were tested in combination with a fuselage, vary in leading-edge sweep from 49° to 74° and the aspect ratio varies from 4.02 to 1.33. All these wings had symmetrical airfoil sections; the 74° swept wing had, in addition, a 15-percent-chord leading-edge flap and a warped section designed for supersonic cruise. The first series of wings had standard 63A and 65A airfoil sections, whereas the second series of wings had flat-plate sections. In this second series of wings, the wings shown in figure 1 on the center right were obtained by removing a portion of the trailing edge from the wings shown on the center left. A portion of the leading edge of these wings could also be changed in order to vary the leading-edge sweep, the leading-edge profile shape, and the wing aspect ratio. The leading-edge profile shape was varied from sharp to nearly round. The thickness for these wings varied between 3 and 5 percent chord.

The wind-tunnel studies were made in the Langley low-turbulence pressure tunnel. Because of tunnel limitations, the Mach numbers were limited to 0.30. As a result, only a brief discussion of Mach number effects is included herein.

Boundary-Layer Transition

For the purpose of insuring turbulent flow on these wings, transition strips were placed on the upper and lower surface of each wing panel. The size and location of the transition particles needed to provide fully turbulent flow rearward of the strips were determined by the methods discussed previously in paper no. 2 by Braslow, Hicks, and Harris.

The significance of fixing transition on a wing surface as regards the drag due to lift is illustrated in figure 2. The variations of the drag with Reynolds number, at lift coefficients of 0 and 0.3, are presented for a wing with fixed and free transition. The transition strips were added near the leading edge of this wing so as to obtain the correct value of drag at zero lift. The transition strip, of course, would not be expected to affect leading-edge separation. These data show that at zero lift and low Reynolds numbers the wing with free transition exhibits a lower value of drag than the wing with fixed transition. As the Reynolds number is increased, the point of natural transition moves forward on the wing with the result that the difference in drag is considerably reduced. At the higher lift coefficient the point of natural transition is presumed to be near the nose of the wing inasmuch as values of drag for this wing are the same as for the wing with fixed transition.

It is evident from these data that the wings with fixed and free transition will exhibit values of drag due to lift which are somewhat different. Therefore, if correct values of drag due to lift are to be obtained, care must be taken to select transition particles of proper size to provide fully turbulent flow over the wing. (See ref. 1.)

Leading-Edge-Suction Parameter

Of the several parameters available for drag-due-to-lift analyses, the one to be used in this paper is the effective leading-edge suction. The definition of this parameter and reasons for its choice are demonstrated in figure 3. This parameter is referred to as "effective leading-edge suction" because, for the highly swept thin wings under consideration, the departure from the full suction theory is associated primarily with leading-edge separation. It should be noted that the subsequent use herein of an effective suction includes all the profile drag due to lift $C_{D,p}$. The drag-coefficient variation with lift coefficient is presented for two flat-plate wings with identical leading-edge shape but of different aspect ratio and taper ratio. The wing on the right of the figure was obtained from the wing on the left by removing a portion of the wing trailing edge.

In both plots, the upper curve is for zero percent suction, and the lower curve is for 100 percent suction. The experimental data are shown by the circular test points. As indicated by the force diagram, the zero percent suction curve corresponds to the condition when the resultant-force vector is normal to the chord, as a result of extensive separation at the wing leading edge. The drag-due-to-lift coefficient for this condition is $C_L \tan \alpha$. For 100 percent suction, the drag-due-to-lift coefficient is the potential flow induced vortex drag and is indicated as $C_{D,i}$ in the vector diagram. The drag-due-to-lift coefficients for 100 percent suction were determined from a modified Multhopp subsonic lifting surface theory. For an elliptically loaded wing this value would be the classic $C_L^2/\pi A$.

The effective leading-edge-suction parameter s is defined as the experimentally measured suction in percent of the total theoretical suction; that is, it locates the experimental data relative to the two theoretical boundaries and is given by the following equation:

$$s = \frac{C_L \tan \alpha - \left(C_D - C_{D,o}\right)}{C_L \tan \alpha - A \int_{-1}^{1} \Gamma \alpha_i \, d\left(\frac{y}{b/2}\right)} \times 100$$

For these wings, the effective suction level is approximately 18 percent and indicates that for these wings with identical leading-edge shape the suction parameter s is independent of aspect ratio and taper ratio.

Another method of analysis based on use of the coefficient of profile drag due to lift $C_{D,p}$ does not show this independence of aspect ratio and taper ratio, as is illustrated in figure 3, where at $C_L = 0.3$, the wing on the right had a $C_{D,p}$ that is 30 drag counts higher than the wing on the left.

Because the leading-edge-suction parameter tends to eliminate the effects of aspect ratio and taper ratio, this parameter s was chosen to analyze the drag-due-to-lift characteristics presented. For the warped wings of this investigation the suction parameter was determined by using a value of $C_{D,o}$ from an equivalent flat wing, whereby camber drag was eliminated from the analysis.

Sharp-Leading-Edge Wings

For supersonic speeds, the requirement for acceptable performance dictates the use of thin highly swept wings, and for a wing with a supersonic leading edge, use of a sharp leading-edge section. A sharp leading edge, of course, is not conducive to low values of drag due to lift at subsonic speeds, as is illustrated in figure 4. The variation of leading-edge suction is presented as a function of Reynolds number for a 67° swept wing in the left plot, and the variation of suction with wing sweep for several sharp-edge wings is shown in the right plot. The values of s shown in this figure and in most of the following figures were taken at the lift coefficient for $(L/D)_{max}$ and are designated $C_{L,opt}$.

These data show that the 67° swept wing exhibits low values of suction, and only a slight increase with Reynolds number is evident. All the sharp-edge wings of the present study, shown as the circular symbols on the right of figure 4, exhibited the same trend of only slight variations of s with Reynolds number that is shown by the data for the 67° swept wing on the left. As a result, the suction parameter can be plotted as a function of wing sweep angle independent of Reynolds number. The data for the 67° swept wing presented on the left of this figure is also included on the right as the solid symbol. The data shown by the square symbols were obtained from references 2 to 5. These data again show that sharp-edged highly swept wings exhibit low values of suction. Even for low values of wing sweep, suction values no higher than about 50 percent are evident.

Configuration Modifications

Several features that can increase the effective suction can be incorporated into a wing design. Two of these features are shown in figure 5. This figure shows the effect of leading-edge flaps and wing warp on the variation of the leading-edge suction with Reynolds number for a 74° swept wing configuration. These data show that both leading-edge flaps and wing warp increase the values of suction over that obtained on the symmetrical, sharp-leading-edge wing. Although an increase in suction was obtained, still only a slight increase with Reynolds number is evident. The suction obtained for the warped wing shows a value of about 40 percent. Since the warping of this wing was designed from supersonic rather than subsonic considerations, values of suction substantially less than 100 percent are not surprising. Further increases in the effective suction can possibly be obtained on the warped wing by incorporating a leading-edge flap; however, the total increment shown for the symmetrical wing may not be obtained for the warped wing.

A third feature that provides increases in the leading-edge suction is use of a wing leading-edge radius. Figure 6 presents the variation of s and $(L/D)_{max}$ with Reynolds number for a highly swept wing with a sharp and a round leading edge. These data indicate that the wing with the round leading edge exhibits large variations of s with Reynolds number, whereas the wing with the sharp leading edge results in relatively constant values of s. The significance of this result in terms of the variation of $(L/D)_{max}$ with Reynolds number for these two wings is shown in the right-hand plot of this figure. The dashed lines represent lines of constant drag due to lift. For the wing with invariant suction the change in $(L/D)_{max}$ with Reynolds number is the result of the change in skin-friction drag. However, for the wing with the round leading edge only about 1/3 of the increase in $(L/D)_{max}$ can be attributed to the reduction in skin-friction drag and the other 2/3 to the reduction in drag due to lift. Tests at supersonic speeds on a wing of sufficient sweep to have the leading edge swept behind the Mach line (i.e., a subsonic leading edge) have indicated that a leading-edge radius of approximately the same percentage of the wing chord as shown in this figure could be added without imposing a loss in performance (ref. 6).

The previous discussion has shown that using the leading-edge-suction parameter tended to eliminate some of the effects of planform in an analysis of the drag due to lift, as long as the conditions at the leading edge of the wing are the same. This result suggests that in attempts to correlate the wind-tunnel data use might be made of a parameter which considers only the leading-edge conditions. The parameter used in this analysis is a Reynolds number based on the velocity component and an average leading-edge radius, both measured normal to the leading edge of the wing. A correlation of the wind-tunnel data by use of this Reynolds number is shown in figure 7. In this figure, the suction parameter s is presented as a function of the leading-edge Reynolds number R_{le}. The data shown are for the symmetrical wings shown in figure 1. These wings have thickness ratios between 3 and 5 percent chord and leading-edge sweep angles between 49° and 73°. These data indicate that about 90 percent suction can be obtained on highly swept thin wings at Reynolds numbers (based on leading-edge radius) above 20 000.

Earlier correlations obtained by using transition-free data have shown somewhat different results, especially in the low Reynolds number range. (See ref. 7.)

Effect of Lift Coefficient and Mach Number

The preceding summary figures have shown the effects of some configuration variables on the leading-edge suction taken at $C_{L,opt}$ and at low Mach numbers.

Several other effects should be considered. The first, which is shown in figure 8, is the variation of suction with lift coefficient for 45° and 62° swept wings at several Reynolds numbers. The data for the 45° swept wing, which were obtained from reference 1, show that increasing the Reynolds number results in an increase in the suction at $C_{L,opt}$, and these high values of suction can be maintained to significantly higher lift coefficients before separation effects cause the suction to diminish. However, for the 62° swept wing, leading-edge separation occurs at relatively low lift coefficients so that even at the higher Reynolds numbers, high values of suction can be maintained over only a small lift-coefficient range. Simple sweep theory would indicate the same effects shown by these data; that is, separation effects causing losses in suction would occur at significantly lower lift coefficients for the highly swept wing. It should be emphasized that because of the large variations of suction with lift coefficient exhibited by these wings, the use of a constant value of suction (for example, the value obtained at $C_{L,opt}$) in defining the entire drag polar would give dangerously optimistic results.

In paper no. 3 of this conference, D. L. Loving suggested that the location of the transition strips can significantly affect the separation characteristics behind the strip. However, for these thin wings at low speeds the large loss of effective suction at the higher lift coefficients is primarily associated with leading-edge separation, and it is not expected that the position of the transition strips would significantly affect these results.

Another effect to be considered is that of Mach number on the leading-edge suction, as shown in figure 9. A search of the literature indicated that data are very scarce from systematic investigations, in the high-subsonic-speed range, of the effects of leading-edge radius, Reynolds number, and wing planform for highly swept wing-body configurations which have transition fixed at the leading edge of the wing. Therefore, only a limited analysis of the Mach number effects, based on the data presented in this figure, is possible. These data were obtained from reference 1. In this figure, the suction parameter is given as a function of Mach number for 45° and 63° swept wings, both wings having 5-percent-thick symmetrical and conically cambered airfoil sections. These data show that the suction varies very slightly with Mach number for the symmetrical wings. However, for the conically cambered 45° swept wing, although substantial improvement is provided at low speeds, losses in suction appear at Mach numbers above 0.7 until at a Mach number near 1.0 the cambered and symmetrical 45° swept wings have nearly the same value of s. For the delta wing, the benefits of camber are maintained to the highest Mach number of the tests because of the high critical Mach number associated with the higher leading-edge sweep angle. The limited results shown are applicable only to these wings, in that changes in the airfoil section or wing planform could significantly alter these results. Additional systematic results are needed to complete this study.

With regard to these Mach number dependent data, it should be noted that for higher lift coefficients, if shock stall is encountered, the method of fixing transition utilized in this study may not provide reliable aerodynamic data, as has been pointed out previously in paper no. 3 by Loving.

CONCLUSIONS

Studies of various factors affecting the subsonic drag due to lift of thin, highly swept wings indicated the following conclusions:

1. Wings having sharp leading edges exhibit low values of leading-edge suction, and no significant change in the suction with increasing Reynolds number is evident.

2. Wings incorporating leading-edge radius exhibit approximately 90 percent suction at Reynolds numbers (based on leading-edge radius) above 20 000.

3. The suction developed by highly swept wings is considerably reduced as lift coefficient is increased, even at relatively high Reynolds numbers; and realistic drag estimates should include this effect.

4. Additional systematic studies are needed for a more comprehensive understanding of the effects of Mach number on leading-edge suction.

REFERENCES

1. Boyd, John W.; Migotsky, Eugene; and Wetzel, Benton E.: A Study of Conical Camber for Triangular and Sweptback Wings. NACA RM A55G19, 1955.

2. Carter, C. Robert: Effect of Rearward Body Strakes on the Transonic Aerodynamic Characteristics of an Unswept-Wing Fighter Aircraft. NASA TN D-3011, 1965.

3. Blackwell, James A., Jr.; and Kelly, Thomas C.: Effects of Configuration Geometry on the Transonic Aerodynamic Characteristics of Canard Airplane Configurations. NASA TN D-2465, 1964.

4. Ray, Edward J.; and Taylor, Robert T.: Transonic Aerodynamic Characteristics of a Tailless Fixed-Wing Supersonic Transport Model. NASA TM X-1214, 1966.

5. Holdaway, George H.; and Mellenthin, Jack A.: Investigation at Mach Numbers of 0.20 to 3.50 of Blended Wing-Body Combinations of Sonic Design With Diamond, Delta, and Arrow Plan Forms. NASA TM X-372, 1960.

6. Morris, Odell A.; and Fournier, Roger H.: Aerodynamic Characteristics at Mach Numbers of 2.30, 2.60, and 2.96 of a Supersonic Transport Model Having a Fixed, Warped Wing. NASA TM X-1115, 1965.

7. Frost, Richard C.; and Rutherford, Robbie: Subsonic Wing Span Efficiency. AIAA J., vol. 1, no. 4, Apr. 1963, pp. 931-933.

SCOPE OF WIND-TUNNEL PROGRAM

$M < 0.30$; $R_{\bar{c}} = 1 \times 10^6$ TO 20×10^6

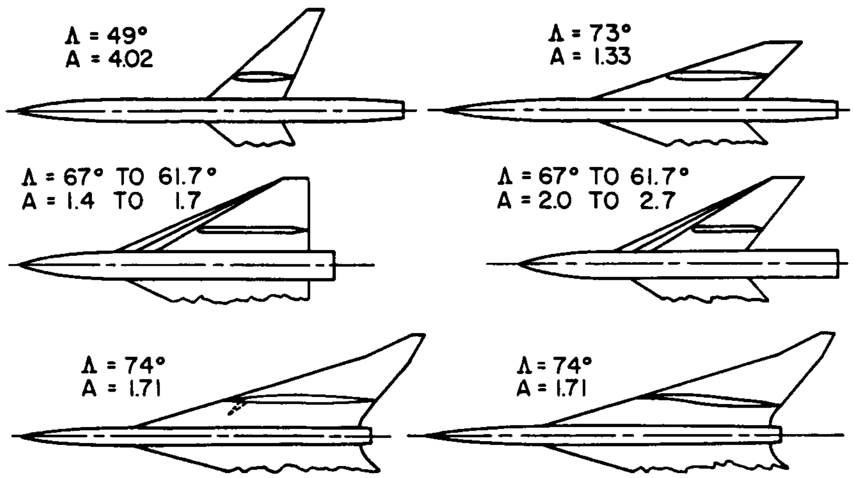

Figure 1

THE EFFECT OF TRANSITION

SHARP LEADING EDGE; $M < 0.30$

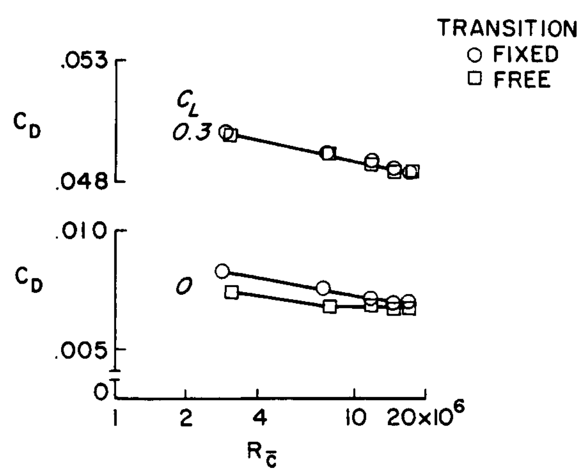

Figure 2

CHOICE OF PARAMETERS

s = MEASURED C_S IN % OF THEORETICAL C_S; M < 0.30

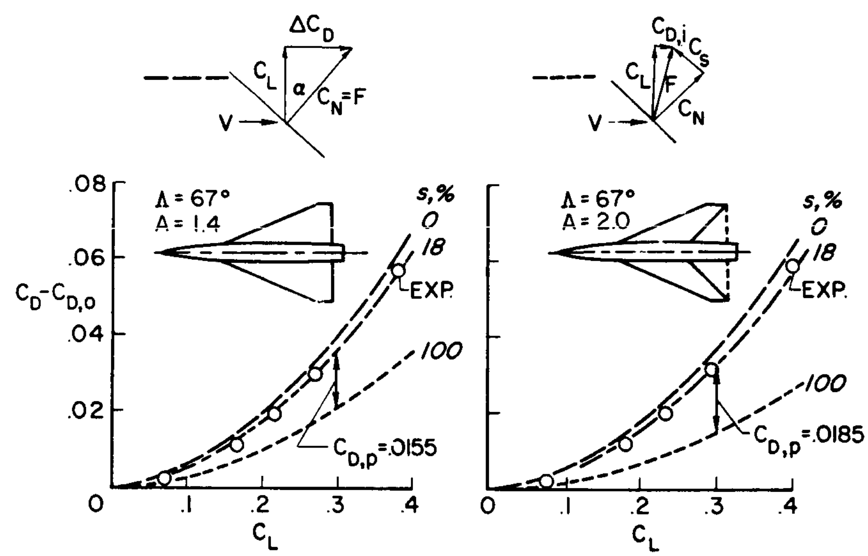

Figure 3

VARIATION OF s WITH $R_{\bar{c}}$ AND Λ

SHARP LEADING EDGES; $C_{L,opt}$; M < 0.30

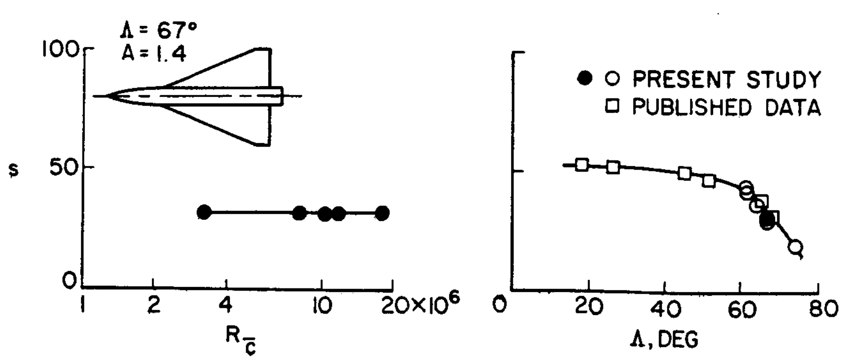

Figure 4

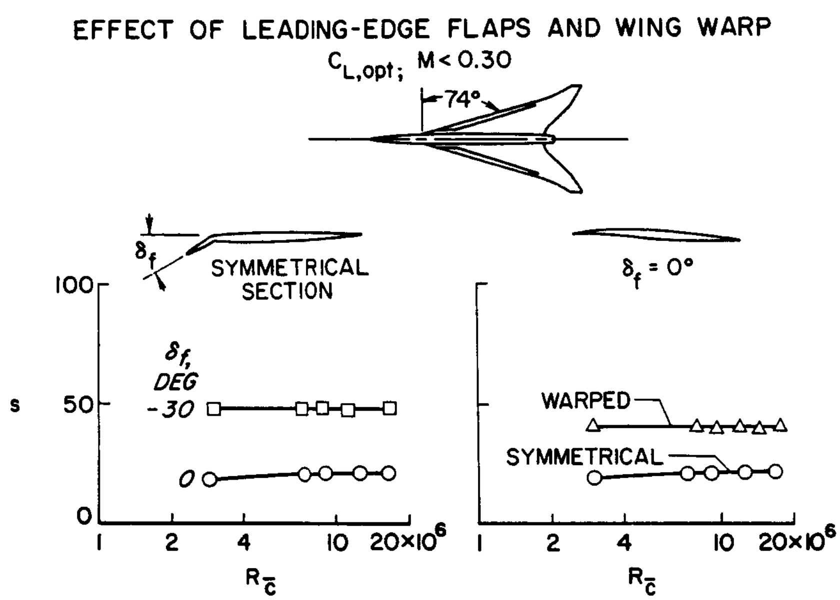

Figure 5

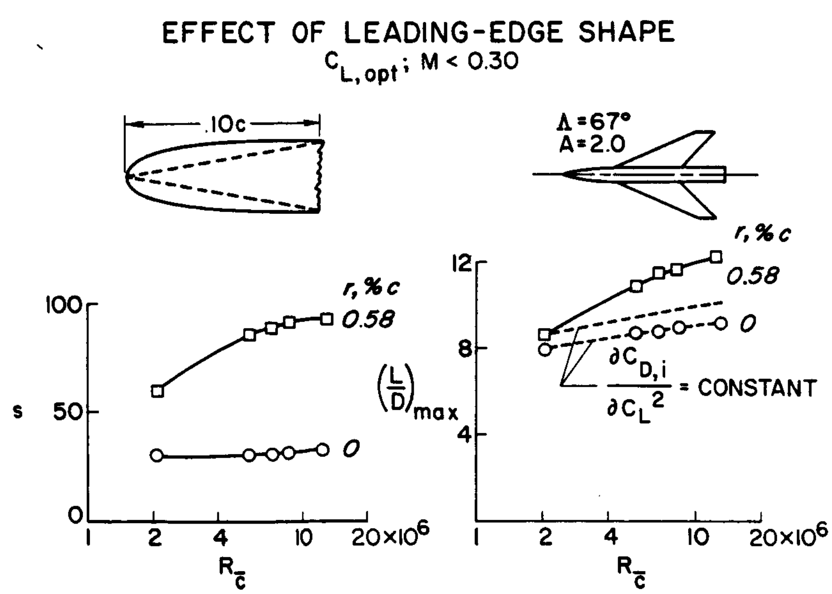

Figure 6

CORRELATION OF s

SYMMETRICAL WINGS; Λ = 49° TO 73°; $C_{L,opt}$; M < 0.30

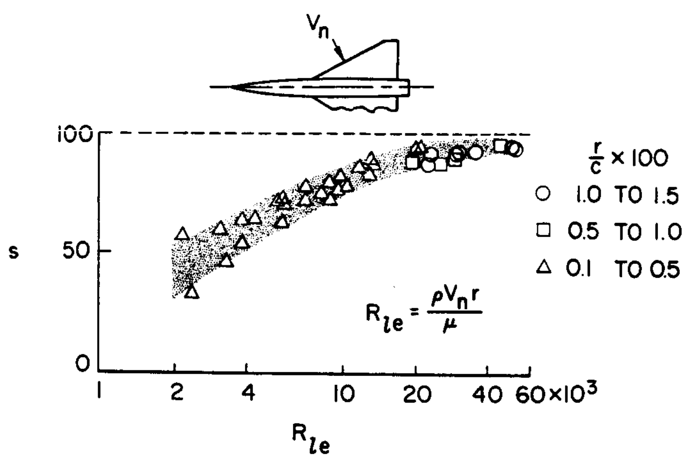

Figure 7

VARIATION OF s WITH LIFT COEFFICIENT

M < 0.30

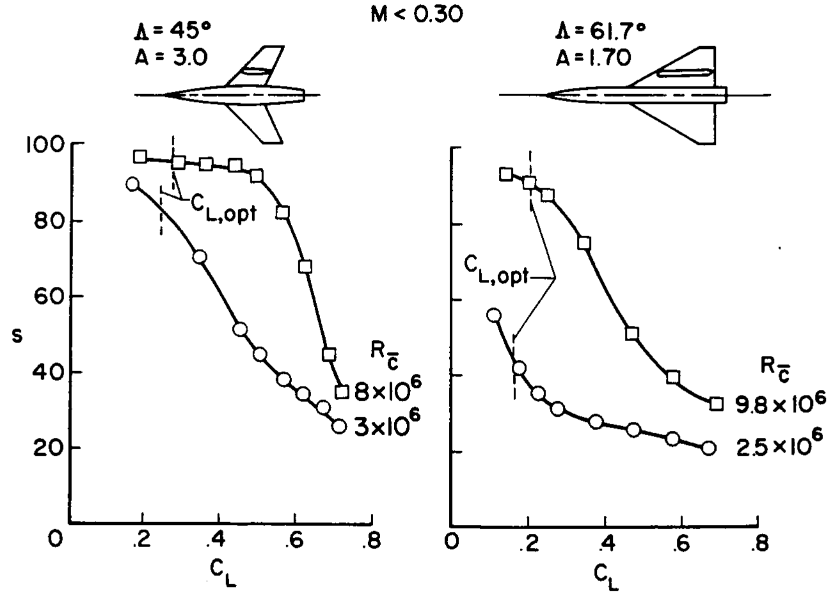

Figure 8

VARIATION OF s WITH MACH NUMBER

$C_{L,opt}$; $R_{\bar{c}} = 2.9 \times 10^6$; $\frac{t}{c} = 0.05$

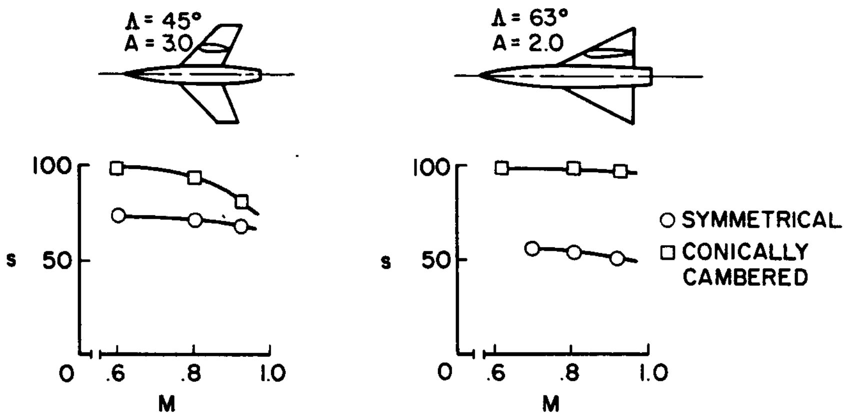

Figure 9